Rotman Lens Performance Analysis

Shruti Vashist[1], Dr. M.K Soni[2] ,Dr.P.K.Singhal[3]

[1]Research Scholar, Department Of Electronics & Communication Engineering, Faculty of Engineering and Technology, Manav Rachna International University Faridabad-121004, Haryana, India

[1]shruti.fet@mriu.edu.in, [2]ed.fet@mriu.edu.in, [3]pks_65@yahoo.com

***Abstract*—This paper presents a trifocal Rotman Lens Design approach. The effects of focal ratio and element spacing on the performance of Rotman Lens are described. A three beam prototype feeding 4 element antenna array working in L-band has been simulated using RLD v1.7 software. Simulated results show that the simulated lens has a return loss of –12.4dB at 1.8GHz. Beam to array port phase error variation with change in the focal ratio and element spacing has also been investigated.**

***Keywords*— Rotman Lens, Array Factor, Return Loss, Phase Error, Beam Steering.**

I. Introduction

Microwave lens has emerged as a beam forming network and is now currently used in many cutting edge applications such as radars, remote satellite sensors, automobile collision avoidance systems and ECM. Different active and passive beam forming networks (BFN's) are known from literature [1], [4]. BFN's which are based on buttler matrix are easy to construct and are also implementable on printed circuit boards, but the major drawback of these BFN's is that the produced beams are dependent on frequency and the beam shift occurs as frequency varies, which is not desirable in most communication links. Hardware complexity of these BFN's grows exponentially with the number of elements and hence it becomes difficult to realize such kind of BFN's for large number of radiation beams. Rotman lens provides an effective solution for beam forming networks when a large number of radiating elements are required. Rotman lens is a true time delay beamformer which provides linear phase shifts at the output ports by utilizing different paths within the lens structure. Rotman lens is a type of microwave lens and is capable of operating in high microwave frequency ranges with wide angle scanning capabilities. It is an Electronically Scanning Antenna (ESA) which has the ability to position the antenna beam instantaneously to any position and can also be implemented in the microstrip configuration. W.Rotman and R.Turner first proposed the rotman lens which consist of airfilled parallel conducting plates fed by co-axial probes [1]. D. Archer[2] gave a modified design of rotman lens in which a dielectric material is filled between parallel conducting plates fed by microstrip lines. Both type of the above mentioned rotman lens have been implemented mostly in the microwave band. At higher microwave frequencies the lens loss increases and there physical structure becomes more difficult to build [3]. Conductor loss is a dominant factor in the overall lens loss and this is due to the increase in the surface resistance at high frequency. At low microwave frequencies it becomes quite difficult to integrate rotman lens realization in compact transceiver designs.

This paper presents the analysis of the effects of variation of antenna element spacing and focal ratio on the performance of rotman lens. Simulations were carried out using RLD1.7 designer software and various important parameters such as array factor, insertion loss, s-parameters, beam to array port phase error, beam to array port coupling magnitude, beam to sidewall coupling magnitude and SWR are analysed to know the effects on the performance of the lens.

This paper is organized as follows: Section II presents the basic principle of the rotman lens in which trifocal lens design equations and its important parameters are discussed. Section III presents the analysis approach of the designed rotman lens and also gives the technical specifications of the designed lenses. In Section IV simulation results are presented and finally in section V conclusions are drawn.

II. Principle of rotman lens

Fig.1 shows a basic diagram of the rotman lens. It consists of a set of input and output ports arranged along an arc. The lens structure between both sets of ports functions as an ideal transmission line between the individual input and output ports. The signal applied to the input port is picked up by the output port. The different electrical lengths between a specific input and all output ports, generates a linear progressive phase shifts across the output ports of the lens. Dummy ports are also an integral part of the rotman lens and serve as an absorber for the spill over of the lens and thus it reduces multiple reflections and standing waves which deteriorates the lens performance[7-9].

A. Lens Design Equation

Fig.2 shows a schematic diagram of a trifocal Rotman lens[12-13]. Input ports lie on contour C1 and the output ports lie on contour C2. C1 is known as beam contour and C2 is known as array contour. There are three focal points namely F1, F2 and F3. F1 is located on the central axis while F2 and F3 are symmetrically located on the array contour at an angle of $+\alpha$ and $-\alpha$ respectively. It is quite clear from Fig.1 that the co-ordinates of two off-axis focal points F2, F3 and one on axis focal point F1 are $(-f_2\cos\alpha, f_2\sin\alpha)$, $(-f_2\cos\alpha, -f_2\sin\alpha)$ and $(-f_1, 0)$ respectively[10][14].

where

f_1 -On axis focal length

f_2 -Off axis focal length

α -Off center focal angle

DOI: 01.IJSIP.5.1.1534

ACEEE Int. J. on Signal and Image Processing , Vol. 5, No. 1, January 2014

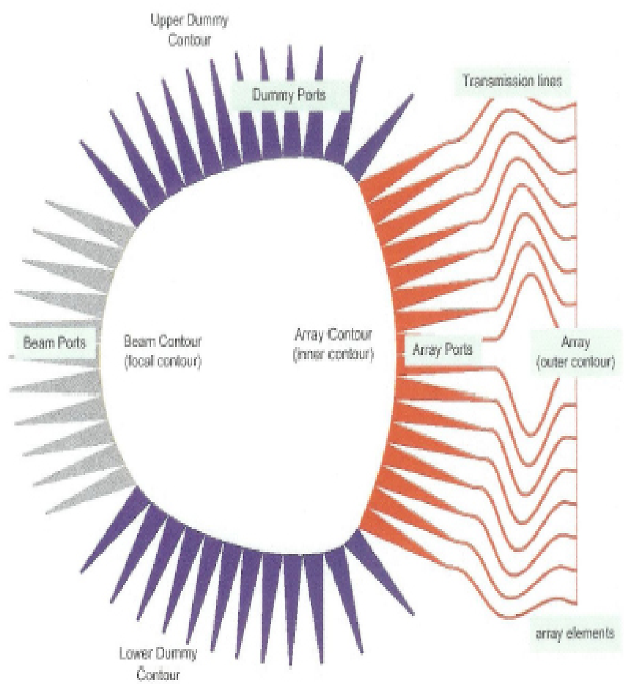

Fig.1 Basic Diagram of Rotman Lens

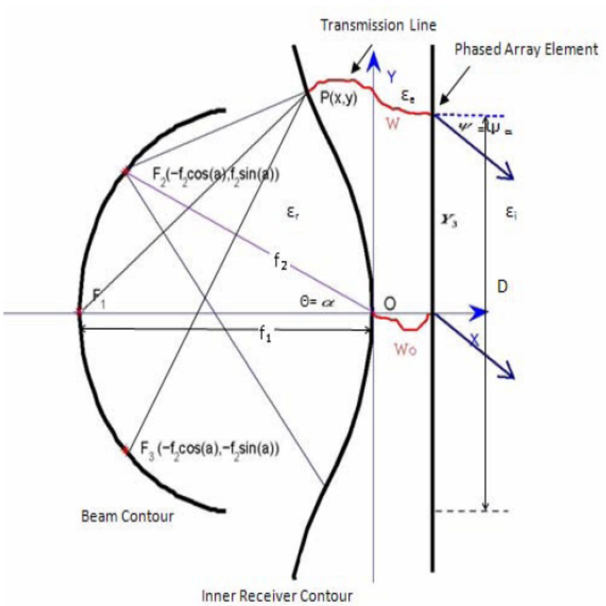

Fig.2 Trifocal Rotman Lens Schematic Diagram

ψ_α -Scanning angle

$\gamma = \dfrac{\sin\psi}{\sin\alpha}$ - beam angle to ray angle ratio given as ratio of sine of their angles.

ε_r -Permittivity of medium in between the lens contour

ε_e - Permittivity of medium of transmission line

ε_i -Permittivity of medium of radiating element

$\beta = \dfrac{f_2}{f_1}$ -Focal ratio

w_o - Transmission line length between axis point 'O' and radiating element.

w -Transmission line length between point 'P' and radiating element.

F_iP-It is the physical distance from focal point Fi to P.

ξ is another important parameter that relates the distance Y_3 of any point on the array contour from the axis, to f_1. ξ controls the portion of phase and amplitude error curves that the lens experiences [4].It is given by-

$$\xi = \frac{Y_3\gamma}{f_1}.$$

If we assume that the ideal focal points are located at $\theta = \pm\alpha$ and 0, and their corresponding radiation angles are $\Psi = \pm\Psi\alpha$ and $\Psi = 0$, given $\Psi\alpha$ is a known angle, simultaneous equations 1-3 are satisfied:

$$F_2P\sqrt{\varepsilon_r} + w\sqrt{\varepsilon_e} + Y_3\sqrt{\varepsilon_i}\sin\psi_\alpha = f_2\sqrt{\varepsilon_r} + w_o\sqrt{\varepsilon_e} \text{------------(1)}$$

$$F_3P\sqrt{\varepsilon_r} + w\sqrt{\varepsilon_e} - Y_3\sqrt{\varepsilon_i}\sin\psi_\alpha = f_2\sqrt{\varepsilon_r} + w_o\sqrt{\varepsilon_e} \text{------------(2)}$$

$$F_1P\sqrt{\varepsilon_r} + w\sqrt{\varepsilon_e} = f_1\sqrt{\varepsilon_r} + w_o\sqrt{\varepsilon_e} \text{-----------(3)}$$

Also we have-

$F_2P^2 = (-f_2\cos\alpha - X)^2 + (-f_2\sin + Y)^2$————————(4)
$F_3P^2 = (-f_2\cos - X)^2 + (-f_2\sin - Y)^2$————————(5)
$F_1P^2 = (f_1 + X)^2 + (Y)^2$———————————————————(6)

By algebraic manipulation of the above equations we can obtain geometric lens equation[10][11] which is quadratic in nature and is given by-

$$aW^2+bW+c=0$$

Where-

$$a = 1 - \frac{(1-\beta)^2}{(1-\beta C)^2} - \frac{\varepsilon_i\xi^2}{\varepsilon_r\beta^2}$$

$$b = -2 + \frac{2\varepsilon_i\xi^2}{\beta\varepsilon_r} + 2\frac{(1-\beta)}{1-\beta\cos\alpha} - \frac{\xi^2 S^2(1-\beta)}{(1-\beta C)^2}\frac{\varepsilon_i}{\varepsilon_r}$$

$$c = -\xi^2 + \frac{\xi^2 S^2}{(1-\beta C)} - \frac{\xi^2 S^4}{4(1-\beta C)}\frac{\varepsilon_i}{\varepsilon_r}$$

DOI: 01.IJSIP.5.1.1534

ACEEE

W -Normalized relative transmission line length

and is given as $W = (\frac{w - w_o}{f_1})$.

S=sinα and C=cosα

It is important to note that the number of beams, number of elements, maximum beam angle and element spacing are known from the system requirement and so the task is to select the optimum values of α , β , γ and f_1/λ [4].

Element spacing d is also very critical as it controls the appearance of grating lobes. The spacing that just admits a grating lobe is given by[7]-

$$\frac{d}{\lambda} = \frac{1}{2 + \sin \Psi_m} \quad \text{——(7)}$$

where Ψ_m is the maximum beam angle.

When a feed is placed at a non focal point then the corresponding wavefront will have a phase error, but for wide angle scanning capabilities it is necessary to place the feed at non focal points[6].

III. Analysis Approach

Rotman Lens is designed using RLD s/w to operate in the frequency band of 1700 MHz- 1900 MHz with the center frequency of 1.8GHz. The lens is analysed to find the effect of element spacing and focal ratio on the performance of Rotman Lens. The height of array contour and feed contour must be almost same in order to couple maximum power from the feed contour to the array contour [5][6]. Taking this fact into consideration the alpha ratio of the designed lens is kept at 0.5

Fig.3 shows the designed Rotman Lens on RLD software.

The specifications of the designed lens are as follows:-

Elliptical lens contour with element spacing = 0.34λ
Operating frequency = 1.8GHz
Scan angle = 30 degree
Alpha ratio = 0.5
No. of beam ports = 3
Flare angle = 12 degree
Focal length = 1.7384 λ

Focal ratio (g) = 1.0

Substrate Thickness = 1.6mm

Loss tangent = 0.001

Substrate dielectric constant = 4.4

IV. Simulation Results

In order to analyse the effect of focal ratio on the performance of the Rotman Lens the element spacing is kept at 0.34 λ and for the analysis of element spacing effect the focal ratio is kept at unity.

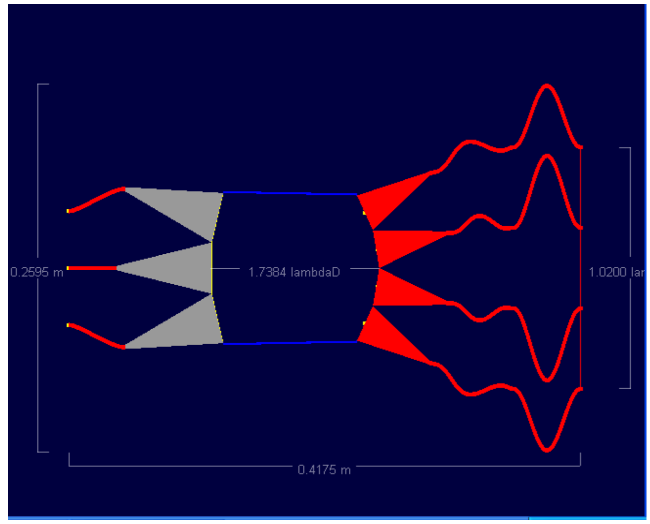

Fig.3 Designed Rotman Lens

A. *Analysis of Array Factor*

Array factor is an important factor for the analysis of Rotman Lens performance. Array factor analysis can indicate the behaviour of side lobe levels and the scanning directions. Fig.4. shows the array factor plot for the element spacing of 0.34 λ.

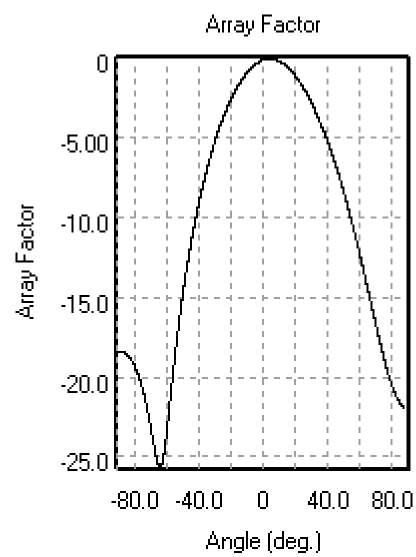

Fig.4 Array Factor with d = 0.34 λ

The side lobe level of less than -15dB for all the frequencies under consideration shows that the performance of the designed lens is very good. Fig. 5 shows the array factor plot for element spacing of 0.7 λ. When the element spacing is increased to 0.7 λ, the number of side lobes and their level both increase which is undesirable. The grating lobe starts to appear which have almost the same level as the main lobe[12][14].

It can also be seen from the above graphs of array factor in fig. 5 that there is a decrease in the width of the main lobe with the increase in the element spacing. Hence it can be concluded that the element spacing should always be kept

DOI: 01.IJSIP.5.1.1534

ACEEE Int. J. on Signal and Image Processing , Vol. 5, No. 1, January 2014

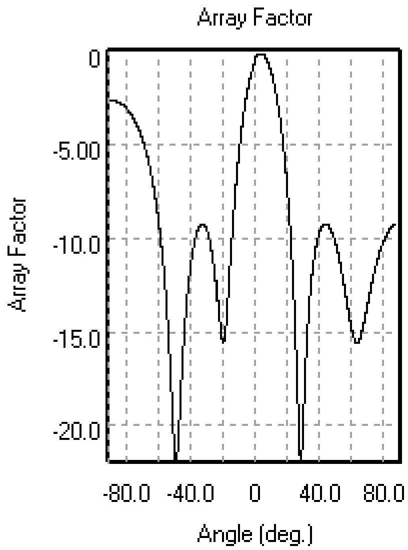

Fig.5 Array factor with d = 0.7 λ

less than 0.5 λ in order to achieve good performance of the lens in terms of the side lobe level and more accurate scanning capability. This result is in good agreement with the element spacing relation given in [4] ie.

$$\frac{d}{\lambda} = \frac{1}{2 + \sin \Psi_m}$$

B. *Beam to array phase error (keeping g constant and varying d)*

TABLE I: BEAM TO ARRAY PHASE ERROR FOR DIFFERENT VALUES OF ELEMENT SPACING

Input Port	Output Port	Phase error in degree d=0.1 λ	Phase error in degree d=0.2λ	Phase error in degree d=0.3λ	Phase error in degree d=0.4λ	Phase error in degree d=0.5λ
2	4	0.020	0.080	0.184	0.330	0.525
2	5	0.00250	0.010	0.025	0.04	0.07
2	6	0.00250	0.010	0.025	0.04	0.07
2	7	0.020	0.080	0.184	0.330	0.525

It is observed from Table I that as the antenna element spacing increases the phase error increases for all the ports due to increased path length difference. It is clearly seen that with 10% increase in the antenna element spacing it is observed that the average beam to array phase error for port 4 increases by 53%.The variation of the phase error due to change in the element spacing can be observed in fig.6.

C. *Beam to array phase error (keeping element spacing constant = 0.34 and varying focal ratio g)*

Fig.7 Shows beam to array port phase error for port 2 excitation at g = 1.0 and element spacing of 0.34 λ. Table II shows the beam to array port phase error for port 2 excitation for different values of **g** (focal ratio). The range over which **g** is varied is 1.0 to 1.1 for the element spacing of 0.34 λ. It can be concluded that increasing the value of **g** will increase the phase error. Maximum phase error is observed for port 4 and port 7 and minimum phase error is for port 5 and port 6. The

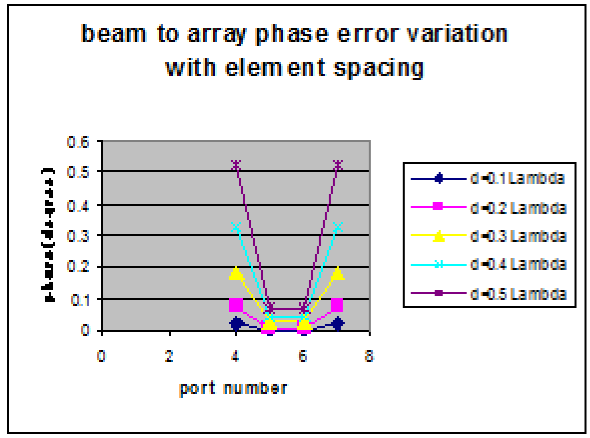

Fig.6 Beam to Array port phase error variation with element spacing

TABLE II: BEAM TO ARRAY PORT PHASE ERROR FOR DIFFERENT VALUES OF FOCAL RATIO 'G'

I/P Port	O/P Port	Phase error in (deg) g = 1.0	Phase error in (deg) G =1.02	Phase error in (deg) g =1.04	Phase error in (deg) g =1.06	Phase error in (deg) g =1.08	Phase error in (deg) g =1.1
2	4	0.237	0.379	0.524	0.672	0.825	0.984
2	5	0.025	0.04	0.05	0.07	0.08	0.10
2	6	0.025	0.04	0.05	0.07	0.08	0.10
2	7	0.237	0.379	0.524	0.672	0.825	0.984

main reason for this is the path length difference. Increasing **g** beyond 1.1 or decreasing **g** below 1.0 for the same simulation set up makes the shape of the lens invalid. Alpha ratio is kept 0.5 so that the height of the array and the beam contour remains almost same, hence maximum power is coupled from beam to array port.

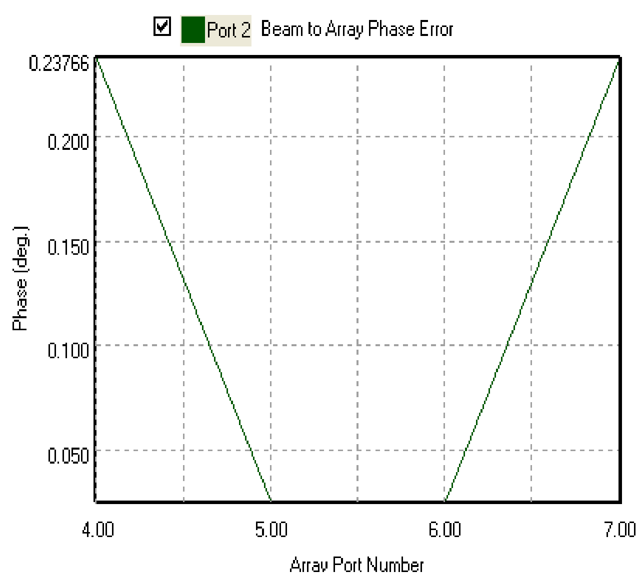

Fig.7 Beam to array port phase error at g = 1.0 and spacing of 0.34 λ

DOI: 01.IJSIP.5.1.1534

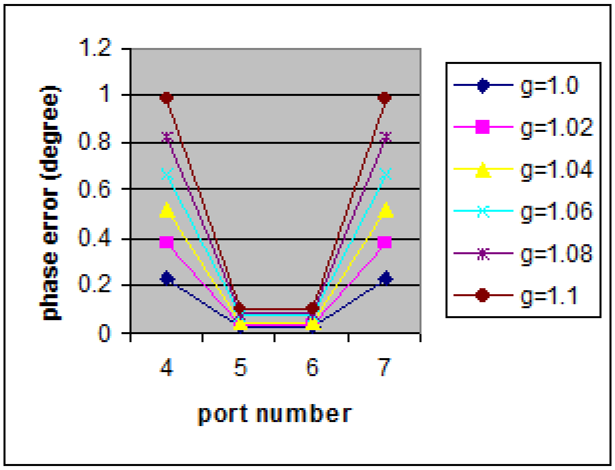

Fig.8 Beam to Array port phase error for different values of focal ratio(g)

Effect of changing 'g' will also change the lens shape, it is found that as g increases the curvature of the feed contour increases and that of the array contour decreases. It has also been observed that changing the focal length also has an effect on changing the contours shape. As the focal length increases the feed contour opens and array contour closes. The effect of variation of phase error with respect to 'g' is shown in fig.8

S-parameters:

S-parameters for the Rotman lens under consideration were also observed .In matrix form the magnitude of S-parameters can be represented as a 3*7 matrix as-

$$\begin{bmatrix} S_{11} & S_{12} & S_{13} & S_{14} & S_{15} & S_{16} & S_{17} \\ S_{21} & S_{22} & S_{23} & S_{24} & S_{25} & S_{26} & S_{27} \\ S_{31} & S_{32} & S_{33} & S_{34} & S_{35} & S_{36} & S_{37} \end{bmatrix}$$

The magnitude at 1.8GHz comes to be

$$\begin{bmatrix} -12.34 & 0 & 0 & -11.60 & -11.44 & -11.37 & -11.22 \\ 0 & -12.34 & 0 & -11.32 & -11.29 & -11.29 & -11.32 \\ 0 & 0 & -12.34 & -11.22 & -11.37 & -11.44 & -11.60 \end{bmatrix}$$

S_{22} magnitude represents the return loss for port 2. Its value is found to be –12.34 dB which shows that only 5.8% of the incident power is reflected back to port 2 and through power is 94.2% . SWR corresponding to this value of return loss is 1.63 and reflection loss is around 0.23dB. Fig.9 shows the plot of magnitude of S_{22} with frequency.

Insertion loss:

The insertion loss is calculated by summing the received powers at the array and beam ports, relative to the transmitted power of each beam. The insertion loss is calculated by-

$$L_k = -10 \log \sum_n |S_{nk}|^2$$

This is the insertion loss corresponding to beam port k where n is the index for the array ports. Fig 10 shows the insertion loss variation for beam port 2 in the operating frequency band .Its value is 6.54dB at 1.8GHz.

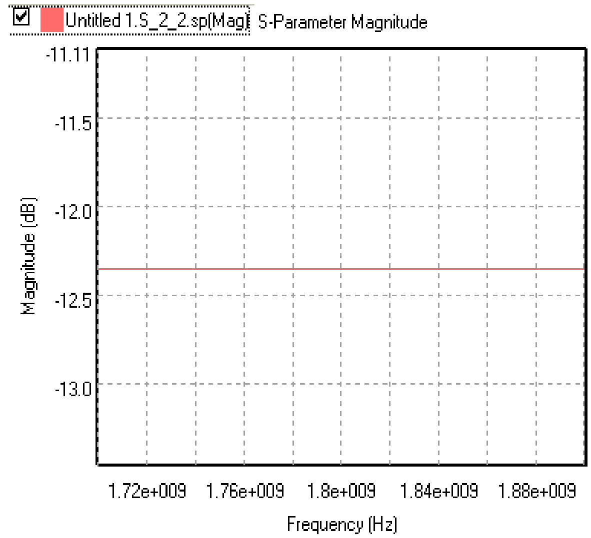

Fig.9. S_{22} plot

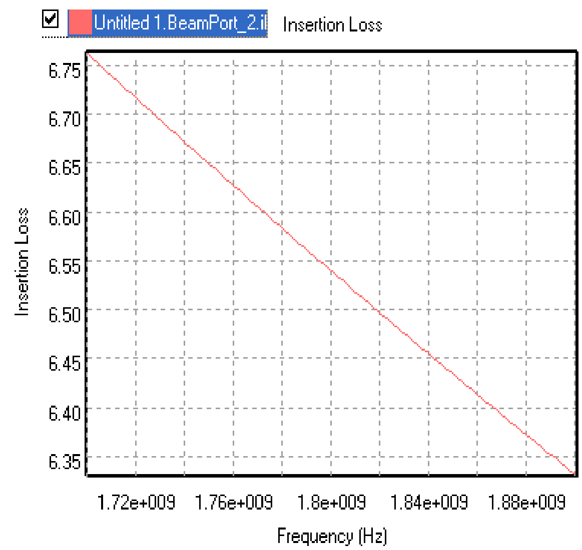

Fig.10 Insertion Loss variation in the operating frequency band

Beam to Array port coupling magnitude:

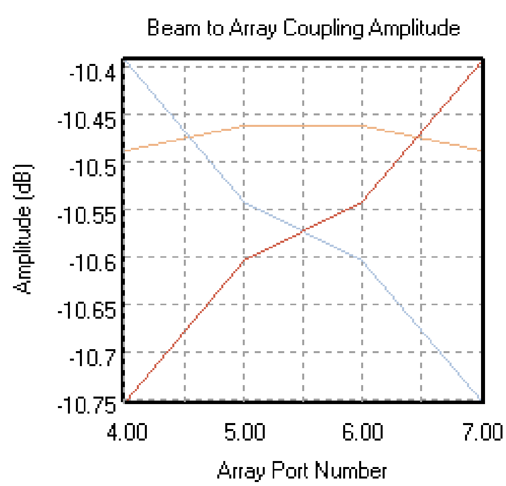

Fig.11 Beam to array coupling magnitude

DOI: 01.IJSIP.5.1.1534

Fig.11 shows the beam to array port coupling magnitude. It can be seen from this graph that the amplitude distribution is nearly uniform for all the array ports for port2 excitation.

Beam to sidewall coupling magnitude:-

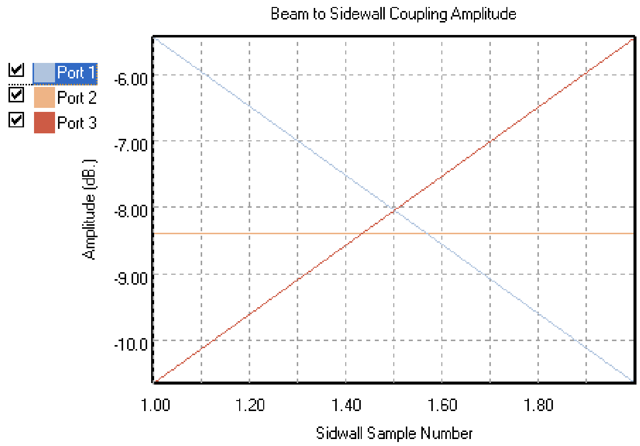

Fig.12 Beam to sidewall coupling magnitude

Fig.12 shows beam to sidewall coupling amplitude for the same simulation set up (port 2 excitation). For **g** =1.0 the beam to sidewall coupling amplitude is found to be -8.4dB.

V. Conclusion

A design approach for trifocal Rotman Lens has been presented in this paper. Rotman Lens prototype with 3 beam ports and 7 array ports has been simulated using RLD1.7 designer software. Simulation results show that element spacing should always be kept below $\lambda/2$ in order to avoid grating lobes in the radiation pattern. Beam to array port phase error increases with the increase in the element spacing and its value is maximum for array ports 4 and 7 at all the element spacings considered. It has been found that with 10% increase in the element spacing it is observed that average beam to array port phase error for port 4 increases by 53%. Focal ratio also affect the beam to array port phase error. It has been found that increasing the value of g increases the phase error and its value is maximum for array port 4 and 7 at all the values of g considered. Increasing g value increases the curvature of feed contour and decreases the curvature of array contour. Analysis of S parameters revealed that the return loss of the designed Rotman Lens is –12.34dB for port 2 (S_{22}) . This indicates that only 5.8% of the incident power is reflected back to port 2 and through power is 94.2%. SWR value and reflection loss are found to be 1.63 and 0.23dB respectively. Insertion loss for beam port 2 excitation for the lens is found to be 6.4 dB at the center frequency of 1.8GHz.

Acknowledgement

Authors would like to thank Mr.Umesh Dutta for his help and support.

References

[1] W. Rotman and R. F. Turner, “Wide angle microwave lens for line source application”, IEEE Trans. 1963, pp. 623-630.
[2] D.H.Archer,”Lens-fed multiple beam arrays”,Microwave J,.PP.171- 95,Sept1984.
[3] J.Kim and F.S.Barns”Dielectric slab Rotman lens with tapered slot antenna array”,IEEE prop-Microwave Antenna Prop.vol.152,no.6,PP.557- 562,Dec 2005.
[4] R.C.Hansen,”Design trades for Rotman lenses”,IEEE Trans Antennas prop vol.39,no.4,April 1991,PP.464-472.
[5] P. K. Singhal, P.C. Sharma, and R. D. Gupta, “Rotman lens with equal height of array and feed contours”, IEEE Transaction on Antennas and Propagation, vol. 51, Issue 8, pp. 2048-2056, Aug. 2003.
[6] P. C. Sharma et al., “Two-dimensional field analysis for CAD of Rotman- type beam-forming lenses,” Int. J. Microw. Millim.-Wave CAD Eng., vol. 2, no. 2, pp. 90–97, 1992.
[7] E. O. Rausch, A. F. Peterson, W. Wiebach: Electronically Scanned Millimeter Wave Antenna Using A Rotman Lens. Radar 97, pp 374-379, October 1997, Publication No. 449
[8] Fuchs H.-H.; Nüßler D’Design of Rotman lens for Beam-Steering of 94 GHz Antenna Array, Electronic Letters 27th May 1999 Vol. 35 No.11.
[9] L. Musa and M. S. Smith, “Microstrip port design and sidewall absorption for printed Rotman lens”, Microwaves, Antennas and Propagation, IEE Proceding, vol. 136, Issue 1, pp. 53-58, Feb. 1989.
[10] T. Katagi, “An improved design method of Rotman lens antennas,” IEEE Trans. Antennas Propag., vol. AP-32, no. 5, pp. 524–527, May 1984.
[11] D. Nußler, H.H. Fuchs, and R. Brauns, “Rotman lens for the millimeter wave frequency range,” in Proc. Eur. Microw. Conf., Oct. 2007, pp. 696–699.
[12] J. Dong, A. I. Zaghloul, and R. Rotman, “Non-Focal Minimum-Phase- ErrorPlanar Rotman Lens,” in URSI National Radio Science Meeting Colorado, 2008.
[13] A. I. Zaghloul and J. Dong, “A Concept for a Lens Configuration for 360-Degree Scanning,” IEEE Letters on Antennas and Wireless Propagation, 2009
[14] J. Dong and A. I. Zaghloul, “Implementation of Microwave Lens for 360-Degree Scanning,” in IEEE International Symposium on Antennas Propagation Charleston, South Carolina, 2009.

DOI: 01.IJSIP.5.1.1534